N-benzylidene-4-dodecylaniline: a New Schiff Base Corrosion Inhibitor for Copper

Lijun Wang[1], Xiaoyan Yin[2,], Weiyun Wang[2], Lei Jin[2], Zhongfang Li[2,*]*

[1] Department of Chemical Engineering, Zibo Vocational Institute, Shandong, Zibo, 255314, PR China
[2] School of Chemical Engineering, Shandong University of Technology, Zibo 255049, PR China
[*]E-mail: Xiaoyanyin731027@163.com; Zhfli@sdut.edu.cn

Schiff base N-benzylidene-4-dodecylaniline (N-bda) was synthesised. The inhibition behavior of the N-bda on the corrosion of copper in a 0.5 mol/L NaCl solution was investigated by SEM, AFM, polarisation curves and electrochemical impedance spectroscopy. SEM and TEM indicate that after N-dba molecules self-assembled on the copper surface, the self-assembled layer protected the metal against corrosion. The maximum inhibition efficiency (*IE*) of N-bda is 98% achieved within 12 h in a 1 mmol/L inhibitor-ethanol solution. The results propose that *IE* increase with the increase of self-assembly time in a certain time range. The adsorption of N-bda on the copper surface occurred via both physical and chemical adsorption following the Langmuir adsorption isotherm.

1. INTRODUCTION

Copper and its alloys are the most common materials in the chemical and microelectronics industries because of their high thermal and electrical conductivities. Copper is a relatively noble metal, requiring strong oxidants for its corrosion or dissolution. Therefore, the protection of copper from corrosion has attracted substantial research attention in the study of corrosion science [1−3].

Self-assembly is a rapidly growing topic in organic chemistry. A previous report indicates that some Schiff base compounds are effective copper corrosion inhibitors in a sodium chloride solution [4, 5]. Schiff bases can be synthesised from relatively inexpensive and simple raw materials. They mainly contain an aromatic ring, an electronegative nitrogen atoms, and unpaired electrons [6].

Over the past few years, several groups have reported a variety of adsorbates on metals with different structures. Such adsorbates include sulfhydryl compound [7], organic thiol [8–10], mercaptoacetic acid [11], amino acids [12, 13], porphyrin [14], phthalocyanine [15], polyvinylpyrrolidone [16], imidazoline [11–19], as well as Schiff bases and their metal complexes [20, 21]. Some Schiff bases that have been reported to inhibit corrosion include thio Schiff bases (IE_{max} = 94%) [22], polydentate Schiff base compounds containing aminic nitrogens (IE_{max} = 94%) [23], tris-hydroxymethyl- (2-hydroxybenzylidenamino)-methane (IE_{max} = 95%) [24], 4-[(4-hydroxy-3-hydroxyl-methyl-benzylidene)-amino]-1,5-dimethyl-2-phenyl-1,2-dihydropyrazol-3-one (IE_{max} = 92%) [25], and 2-[2-(2-(3-phenylallylidene)hydrazine carbonothioyl)- hydrazine- carbonyl]benzoic acid (IE_{max} = 97%) [26]. These Schiff base compounds generally contain N, O and S atoms. However, they have complex structures that make their self-assembled films imperfect. In Schiff bases, unpaired electrons and benzene ring atoms produce more than one centre of chemical adsorption action. Hence, a Schiff base can form a stable chelate with copper [27].

In the current work, a new kind of Schiff base, N-benzylidene-4-dodecylaniline (N-bda), was synthesised. N-bda contains a relatively long chain, which was used as a hydrophobic group [25, 28–30] and left only the –CH=N– groups available for adsorption on the copper surface.

To the best of our knowledge, the use of N-bda as a corrosion inhibitor has never been reported. The relatively long chain of N-bda leaves only the –CH=N– group available to link the entire molecule to the copper surface, in which case chemical adsorption would be likely. In the present study, N-bda was synthesised from benzaldehyde and 4-dodecylaniline. The electrochemical impedance test and polarisation curve measurements were used to examine the inhibitive action of N-bda towards copper corrosion in NaCl solutions. Fourier-transform infrared (FT-IR) spectroscopy, scanning electron microscopy (SEM) and atomic force microscopy (AFM) were used to examine the morphology of the self-assembled copper and blank copper sheet. The activation parameters influencing the inhibition behaviour of N-bda were calculated and the factors affecting the self-assembly were discussed.

2. EXPERIMENTAL

2.1 Chemical materials

Benzaldehyde (Aldrich), 4-dodecylaniline (Aldrich) and other chemicals used in the experiment were commercially obtained and used without further purification. All chemicals were analytical grade. The necessary aqueous solution concentrations were obtained by dissolving relevant chemicals in ultrapure water. Electrochemical measurements were performed in a 0.5 mol/L NaCl solution.

2.2 Preparation of Schiff base

N-bda was synthesised in the laboratory from benzaldehyde and 4-dodecylaniline. 4-Dodecylaniline (2.624g, 0.01 mol) dissolved in ethanol (25 mL) was added to benzaldehyde (0.9500 g,

0.009 mol) also dissolved in ethanol (25 mL). The mixture was allowed to react for 3 h in condensing circumfluence equipment. The temperature was maintained at 35~40 °C for 3 h, during which continuous stirring was performed. After the 3 h reaction, the reaction mixture was heated to half the volume. The solution was then cooled down to crystallise overnight. After filtering, the recrystallisation product was dried at 40 °C. The melting point of the synthetic compound was determined as 47.9 °C via a digital melting point apparatus (WRS-1B). The compound was dissolved in absolute ethanol to the desired concentrations (0.01 mol/L, 1 mmol/L, 0.1 mmol/L, 0.01 mmol/L).

2.3 Preparation of electrodes and self-assembled films

The copper electrodes were prepared according to literature [31]. The working electrodes were prepared from round copper rods 6.08 mm in diameter and 2~3 cm long. Copper sheets were used as the substrate for the SEM, AFM, and FT-IR experiments. After scales or other depositswere removed using acids, epoxide resin and ethylenediamine were used to pack the surface of the copper rods. Ultimately, only the cross-section was left to contact with the electrolyte solution.

The surfaces of the copper electrodes and sheets were ground with silicon carbide abrasive papers (#800 to #2500), and were polished with alumina paste (0.05 μm) to achieve a mirror finish. The surfaces were rinsed with ultrapure water, degreased with acetone, dried in a stream of nitrogen, and etched in a 7 mol/L HNO_3 for 15 s to obtain a fresh copper surface. The copper surface was rinsed with ultrapure water and immediately immersed prepared solutions for designated times. The copper materials were then taken out, rinsed with ultrapure water, and dried with nitrogen. Finally, the copper electrodes were places in a three-electrode cell for electrochemical measurements, and the copper sheets were used for surface topography analyes.

2.4 Electrochemical measurements

Electrochemical experiments were performed in a 150 mL three-electrode electrochemical cell. The copper electrode was used as working electrode. One copper sheet was immersed in a 0.5 mol/L NaCl solution for 6 h. The other was submerged in a 1 mmol/L N-bda solution for 12 h. After that, it was taken out, washed with distilled water, dried with nitrogen, immersed in a 0.5 mol/L NaCl solution for 6 h, washed with distilled water thoroughly, dried with nitrogen. A platinum slice (about 1 cm^2) was used as the auxiliary electrode. A saturated calomel electrode (SCE) was used as the reference electrode, against which all potentials were measured. The electrochemical experiments were carried out using the electrochemical measurement system Potentiostat Model 263A workstation (PerkinElmer) with a lock-in amplifier (10 mHz ~100 kHz; Model 5210, PerkinElmer). Data were collected and figures were plotted using the software Powersuit.

Electrochemical impedance spectroscopy (EIS) measurements were performed at the corrosion potential within the frequency range of 100 kHz to 10 mHz, with 30 points per decade. The amplitude of the sinusoidal perturbation signal was 10 mV at the corrosion potential. The impedance data were

analysed using the ZSimpWin software and were fitted to the appropriate equivalent circuits. The fitting results gave the element parameters in the equivalent circuits.

Polarisation curves were constructed within the potential range of ±0.25 V versus open circuit potential (OCP) at a scan rate of 0.1660 mV/s.

2.5 Fourier-transform infrared (FT-IR) spectroscopy

FT-IR spectra from the N-bda sample and modified copper sheet tested on a Nicolet 5700 Fourier transform infrared spectrometer (Thermo Electron). About 200mg of IR spectroscopic grade KBr was used with 1 mg of the sample. One copper sheet was immersed in 1 mmol N-bda solution for 12 h. Then it was taken out, washed with ethanol and distilled water, dired with nitrogen. The copper sheet was measured with reflectance spectra. FT-IR spectra was obtained in the range of 400~4000 cm^{-1} at room temperature.

2.6 Scanning electron microscopy (SEM)

Two copper sheets samples were prepared as described above (Section 2.3). One copper sheet was immersed in a 0.5 mol/L NaCl solution for 6 h. The other was submerged in a 1 mmol/L N-bda solution for 12 h. After that, it was taken out, washed with distilled water, dried with nitrogen, immersed in a 0.5 mol/L NaCl solution for 6 h, washed with distilled water thoroughly, dried with nitrogen. The copper sheets morphology was investigated using a scanning electron microscope (FEI Sirion 200).

2.7 Atomic force microscopy (AFM) measurement

AFM experiments were performed in the standard mode with a commercial AFM Instrument, Multimode NS3a (Veeco company, America).

Two copper steel samples were prepared as described above (Section 2.3). One copper sheet was immersed in a 0.5 mol/L NaCl solution for 6 h. The other was submerged in a 1 mmol/L N-bda solution at room temperature for 12 h. After that, it was washed with distilled ethanol and water, dried with nitrogen. Then the specimens were used for AFM measurements.

3. RESULTS AND DISCUSSION

3.1 FT-IR spectra

The FT-IR spectrum of the N-bda (Fig.1) manifested the following absorption bands: 3060 and 3029.cm^{-1} (=C–H); 1505, 1467, and 1450 cm^{-1} (C=C rocking); 688 and 749 cm^{-1} (monosubstitution of the benzene ring); 2953, 2918 and 2849 cm^{-1} (CH_{st}), 1362 cm^{-1} (CH_2 deformation), as well as 1625 cm^-

[1] (–C=N) [33].The FT-IR spectrum of copper modified with N-bda contained the same structures as that of N-bda: 2925 and 2852 cm^{-1} (CH$_{st}$); 1666 cm^{-1} (–C=N); as well as 788 cm^{-1} (monosubstitution of the benzene ring). The FT-IR spectra were similar with the synthetic compound. It can be concluded that the N-bda molecules adsorbed on the copper surface.
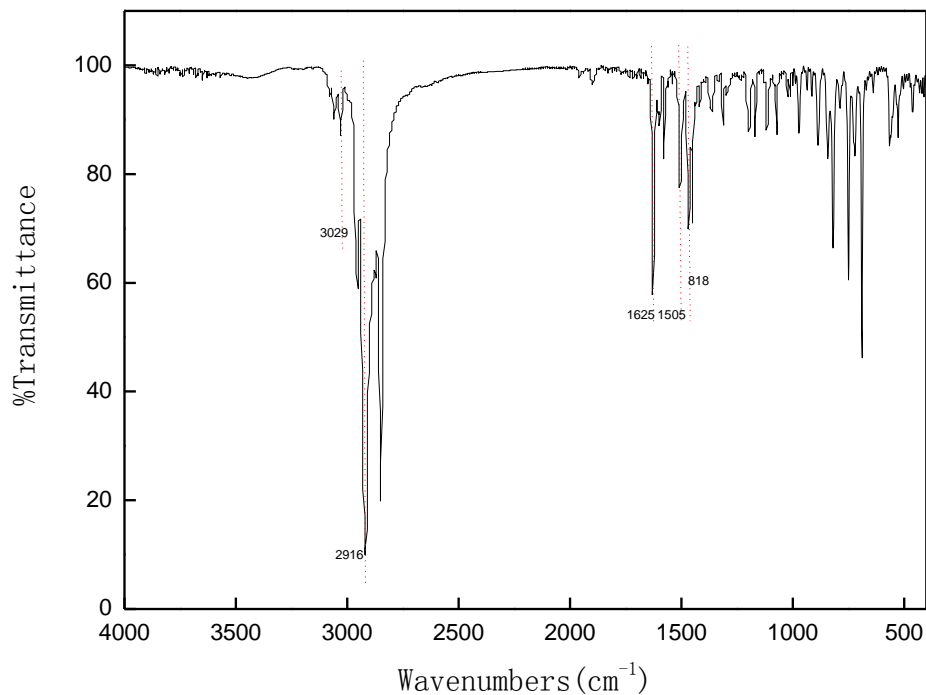
**Figure 1.** The FT-IR spectrum of the N-bda
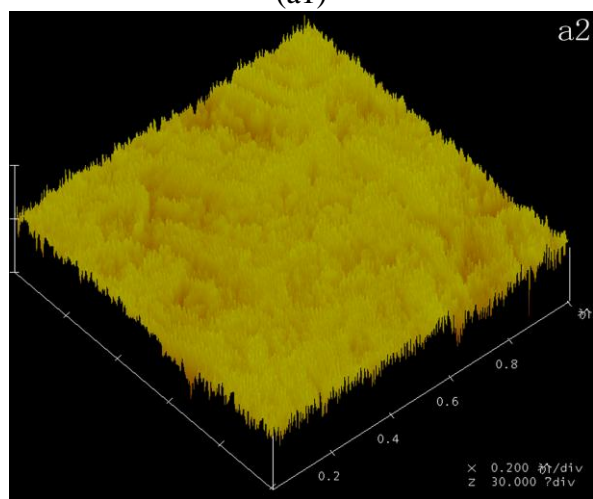
3.2 Scanning Electron Microscopy (SEM)
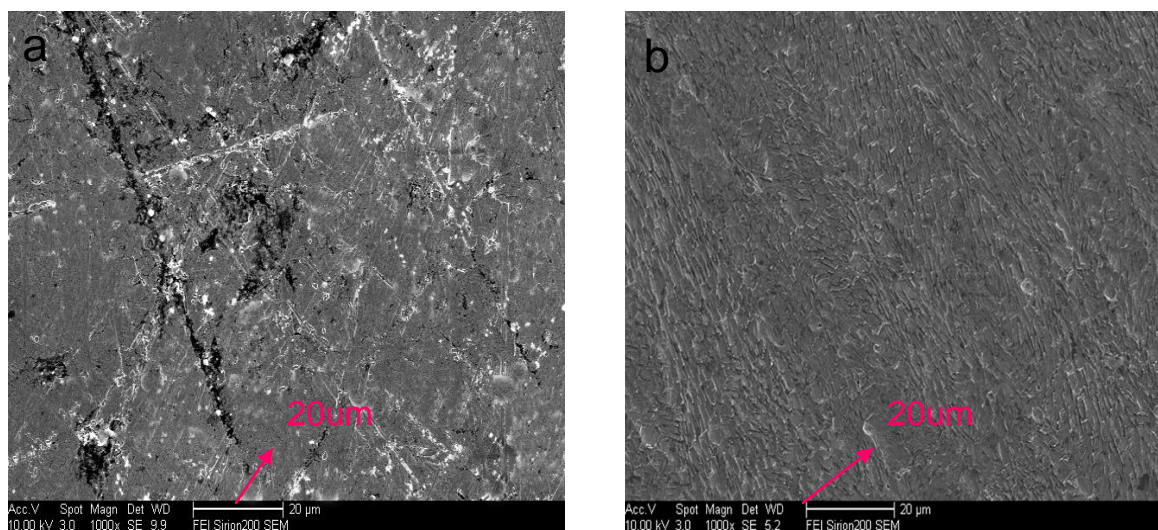
Figure 2. SEM of copper surfaces: (a) copper sheet immersed in a 0.5 mol/L NaCl solution for 6 h; (b) copper sheet immersed in the Schiff base solution for 12 h then immersed in a 0.5 mol/L NaCl for 6 h

Fig.2 shows the scanning electron microscopy (SEM) of the copper sheets. As it shown in Fig. 1a, the blank copper sheet was damaged due to the metal dissolution in a 0.5 mol/L NaCl solution. However, the appearance of copper surface that self-assembled in N-bda-ethanol solution is different. It can be seen from Fig. 1b that the dissolution rate of copper reduced and the smooth surface appear by formation of a protective film on the metal surface. It indicates that N-dba molecules self-assembled on the copper surface, and the self-assembled films can inhibit copper from corrosion.
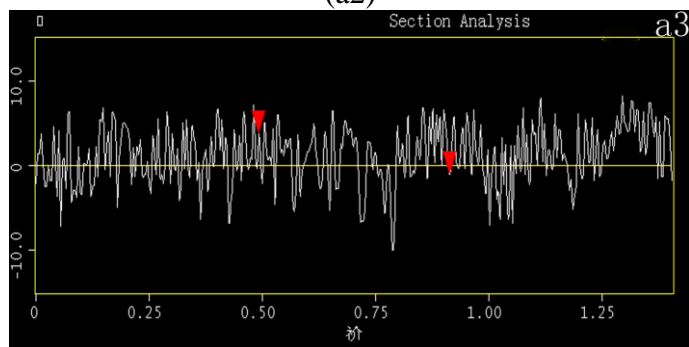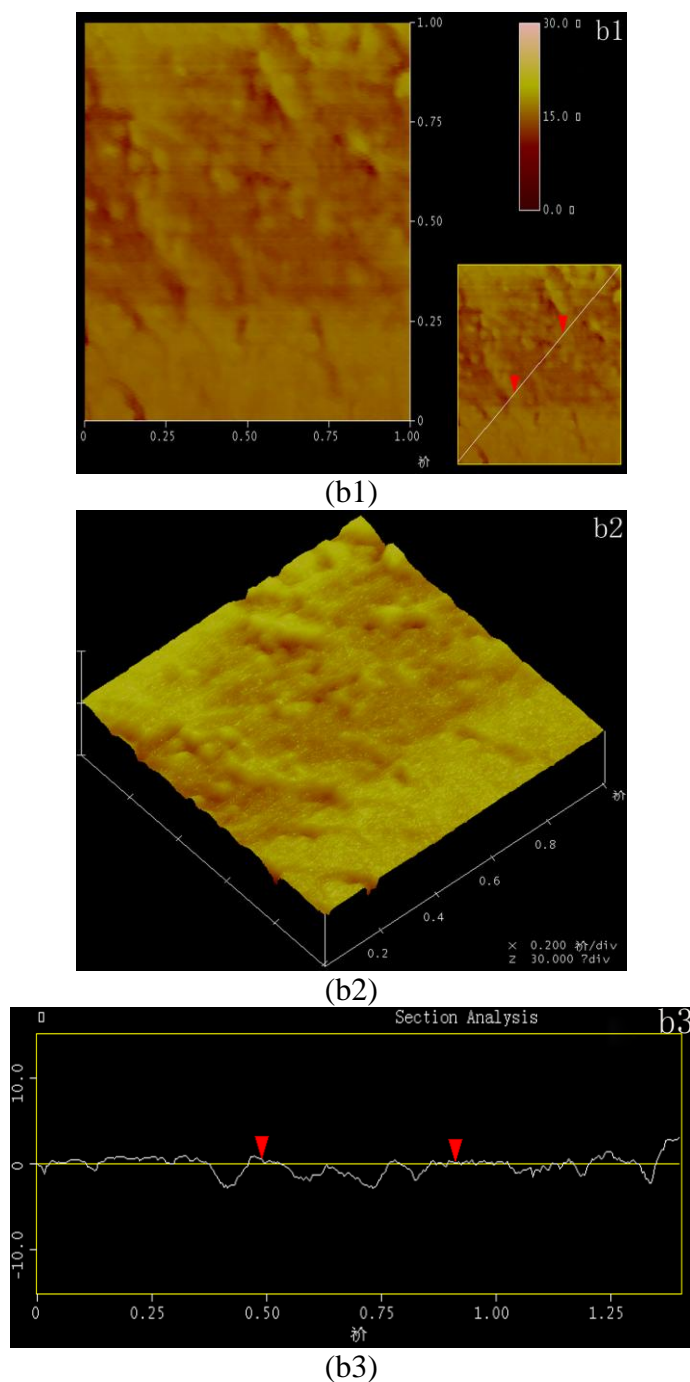
3.3 Atomic force microscopy measurement

(a1)

(a2)

(a3)

(b1)

(b2)
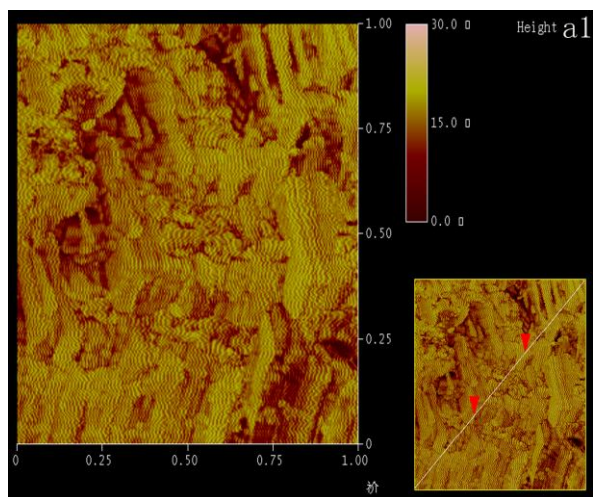
(b3)

Figure 3. 2D (a1, b1), 3D (a2, b2) AFM images, and sectional analysis (a3, b3) of copper sheet: (a) copper sheet immersed in a 0.5 mol/L NaCl solution for 6 h; (b) copper sheet immersed in the Schiff base solution for 12 h then immersed in a 0.5 mol/L NaCl for 6 h

Atomic force microscopy (AFM) offers extraordinarily high resolution images related to force measurement applications. The two (2D) and three-dimensional (3D) AFM images as well as a section analysis of copper surface after exposed to corrosion solution is given in Fig. 2. As it is shown in Fig. 3(a3), the surface of blank copper sheet exposed to corrosion solution is much more rough (roughness 500nm) compared with that of self-assembled copper sheet (15nm) in Fig. 2(b3). The surface of self-assembled copper sheet is much smooth, which suggest N-bda molecules adsored on the copper

surface and reduce copper dissolution. The self-assembled films protected the metal against corrosion. The AFM images of copper are in good agreement with the SEM results.

3.4 Polarization measurements
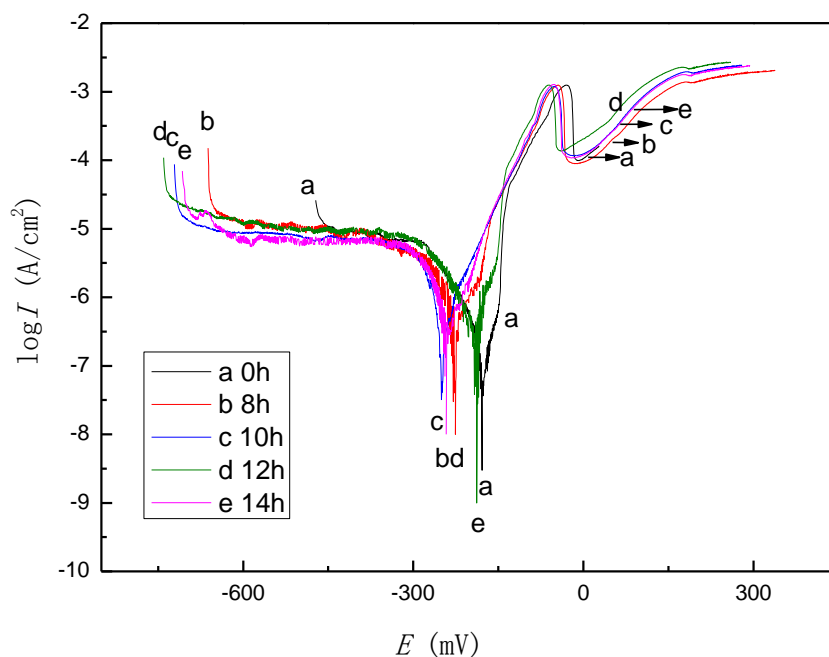
Figure 4. Anodic and cathodic polarization curves for copper electrodes (self-assembly in different times) in a 0.5 mol/L NaCl solution at room temperature

Table 1. Polarization measurement results for copper in a 0.5 mol/L NaCl in different time of N-bda-ethanol solution

Concentration ($mol \cdot L^{-1}$)	time (h)	E_{corr} (mV)	j_{corr} ($\mu A \cdot cm^{-2}$)	*IE* (%)
	0	-179.0	2.192	-
	4	-208.5	0.882	59.8
	6	-241.0	0.612	72.1
	8	-225.5	0.578	73.6
1.00 mmol/L	10	-250.0	0.410	81.3
	12	-188.0	0.0390	98.2
	14	-242.0	0.382	82.6
	16	-248.0	0.528	75.9

Fig. 4 shows the polarization curves for copper self-assembled in different times in the N-bda-ethanol solution, measured in a 0.5 mol/L NaCl solution. Polarization parameters of copper corrosion in a 0.5 mol/L NaCl solution in the presence and absence of N-bda self-assembled films and the corresponding corrosion efficiency are given in Table 1. As expected, corrosion current density (j_{corr})

decreased with increased self-assembly time within 12 h. This result suggested that inhibitor molecules absorbed on the clean copper surface and prevented the copper dissolution. The corrosion rate reduced. When the time is longer than the 12h, the j_{corr} increased. It suggests that the fall off of the adsorb Schiff base molecules, then the corrosion rate increased.

The corrosion current density obtained from the bare copper electrode was 2.191 μA/cm^2 in a 0.5 mol/L NaCl solution. The calculated percent inhibition efficiency (*IE*) was calculated [32] from the following equation:

$$IE(\%) = \frac{j_{corr}^{\circ} - j_{corr}}{j_{corr}^{\circ}} \times 100 \qquad (1)$$

where j_{corr}° and j_{corr} are the corrosion current density values without and with N-bda, respectively.

The anodic reactions of copper in the NaCl solution are:

$$Cu + Cl^- \rightarrow CuCl + e^- \qquad (2)$$
$$CuCl + Cl^- \rightarrow Cu\,Cl_2^- \qquad (3)$$
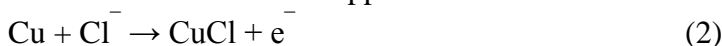
The cathodic dissolution of copper in NaCl solution is as follows:

$$4H^+ + O_2 + 4e^- \rightarrow 2H_2O \qquad (4)$$

The total copper corrosion reaction in NaCl solution is:

$$2Cu + 4H^+ + 4Cl^- + O_2 \rightarrow 2Cu^+ + 4Cl^- + 2H_2O \qquad (5)$$

When solid copper dissolves, copper ions chelate with Cl$^-$. The existence of Cl$^-$ ions subsequently speeds up the dissolution of copper. Fig. 4 shows that the anodic polarization is obviously greater than that of the cathode. E_{corr} of the bare copper electrode is -179.0 mV, and j_{corr} is 2.192 μA/cm^2 (Table 1). When the copper electrode self-assembles in the N-bda-ethanol solution, E_{corr} increases with increasing solution concentration, whereas j_{corr} decreases. As a result, N-bda molecules could inhibit Cl$^-$ from corroding copper.

The best inhibition efficiency was 98.2%, when the copper electrode self-assembled for 12 h in the Schiff base solution (Table 1). The self-assembled films caused the change in the copper electrode surface, which subsequently changed j_{corr} and the E_{corr}. In contrast, there was no definite trend in the shift of the E_{corr} values. It indicated that N-bda is better in inhibiting copper against corrosion than other inhibitors reported under the same conditions.

Addition of Schiff base caused more negative shift in corrosion potential especially in longer time. The behavior of the inhibitor at anodic potentials may be the result of significant dissolution of the copper surface, leading to desorption of the adsorbed inhibitor from the electrode surface. Both anodic and cathodic reactions were effected by increasing the immersion time of copper in the Schiff base solution.


3.5 Electrochemical impedance measurements

The inhibition efficiency (*IE*) in relation to charge transfer resistance was calculated [33] by the following equation:

$$IE(\%) = \frac{R'_{ct} - R_{ct}}{R'_{ct}} \times 100 \qquad (6)$$

where R_{ct}' and R_{ct} are the charge transfer resistances observed in the presence and absence of N-bda, respectively. The values of R_{ct} obtained from impedance measurements increased with prolonged self-assembly time, which can be ascribed to an equivalent increase in the electrode surface area. The self-assembled films could also have stopped the electron transfer from the copper surface to the solution.

The impedance data were analysed using the ZSimpWin software, and they were fitted to the appropriate equivalent circuits. Fig. 5 is the bode plots of self-assembled films covered copper electrode. The copper electrodes were self-assembled for different time in a 1 mmol/L N-bda-ethanol solution. From the Bode diagrams we can deduce the equivalent circuit diagram to fit the impedance spectra. Fig. 6 shows the equivalent circuit. R_s is the solution resistance between the reference electrode and working electrodes. Q_{dl} is constant phase elements modeling the double-layer capacitance (C_{dl}). R_{ct} is the charge transfer resistance corresponding to the corrosion reaction at the metal substrate/solution interface. W is theWarburg impedance attributed to mass transport in the process of the corrosion reactions [31, 33, 34].
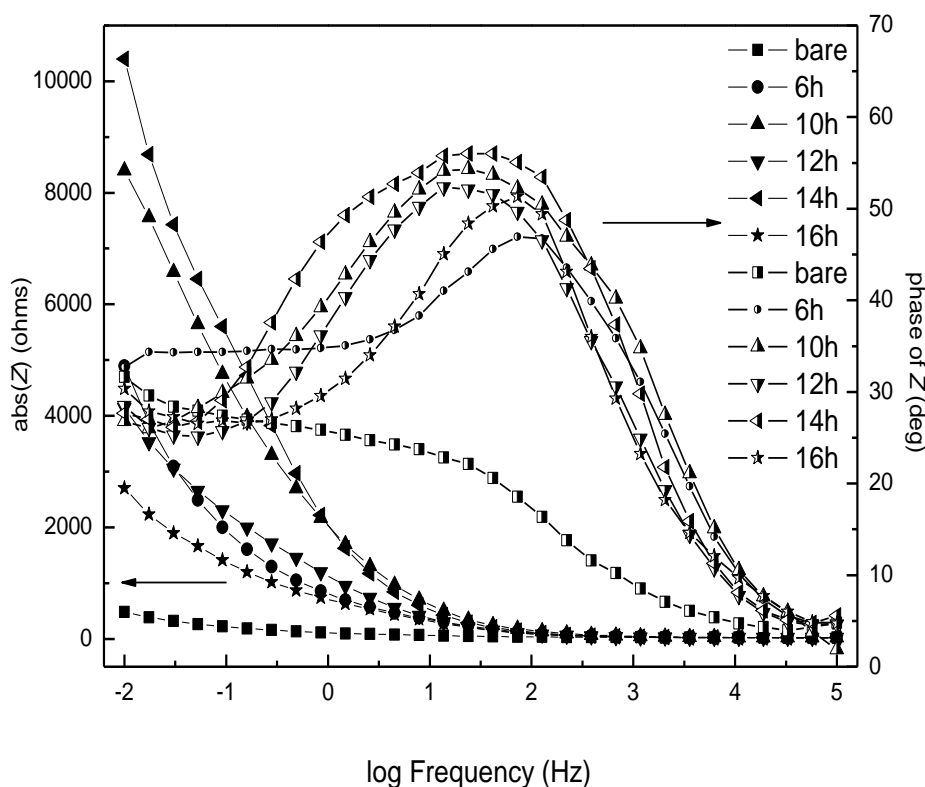

Figure 5. Bode plots of self-assembled films covered copper electrodes in different time of N-bda-ehanol solution, measured in a 0.5 mol/L NaCl solution in the room temperature
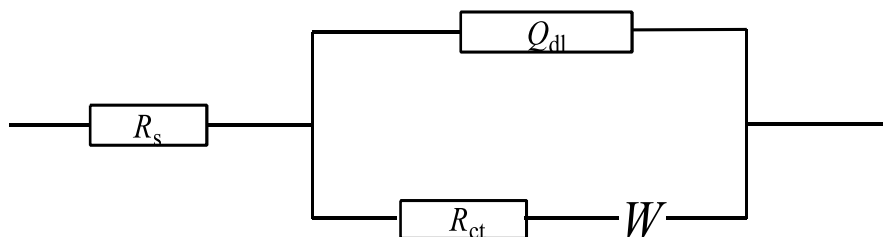
Figure 6. Equivalent circuits for copper electrode modified with or without the N-bda.

Fig. 7 display the impedance diagrams of the copper electrode without or with self-assembled films that self-assembled in different times. In the present of N-bda, the impedance values of the copper electrode increased, especially at low frequencies (*LF*). With the increase of the self-assembly time, the charge transfer resistance (R_{ct}) increased until the time reached to 12 h. The straight line at the low frequency corresponded to the Warburg impedance, which illustrated that there existed a diffusion process between the electrode and the solution. The present of the Warburg impedance (W) characters in the circuit confirms that the mass transport was limited by the surface adsorbed film. The circular curve on the Nyquist plots of the copper electrode appeared at the high frequency (HF) referred to the capacitive loop caused by the relaxation time constant of the charge transfer resistance (R_{ct}). The value of R_{ct} obtained from the fitting software, was equal to the diameter of the capacitive loop [35, 36]. When the time was higher than 12 h, the Rct values decreased with the time increased.
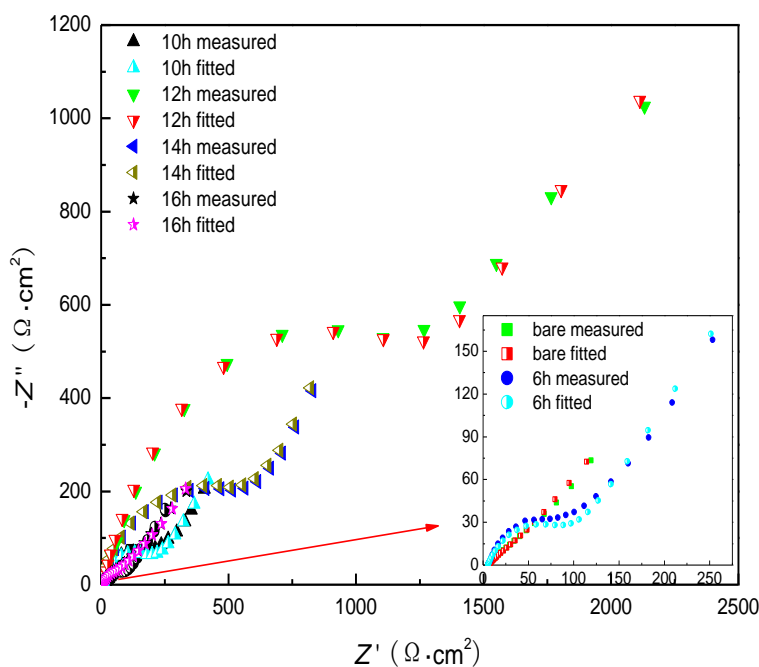

Figure 7. Nyquist plots for the copper electrodes self-assembled in different times in Schiff base-ethanol solution

Table 2. Impedance parameters for copper electrode with self-assembled films formed in different times in a 0.5 mol/L NaCl solution

time (h)	R_s ($\Omega \cdot cm^2$)	Q_{dl}		R_{ct} ($\Omega \cdot cm^2$)	W (Ω)	IE (%)
		Y_0 ($\Omega^{-1} \cdot cm^{-2} \cdot s^n$)	n(0-1)			
bare	5.8	0.0155	0.4	138.7	0.0126	
6	5.5	608×10^{-4}	0.8	925.6	0.0172	85.0
10	6.2	3.59×10^{-4}	0.8	1175	0.00198	88.2
12	6.1	5.24×10^{-4}	0.8	6237	0.00486	97.8
14	5.5	9.14×10^{-4}	0.8	1234	0.0140	88.8
16	5.6	5.07×10^{-4}	0.8	259.7	0.00606	46.6

The impedance quantitative results can be seen in Table 2. It is clear that, the corrosion of copper is obviously inhibited in the presence of the inhibitor. R_{ct} values increased from 138.7 $\Omega \cdot cm^2$ to 6237 $\Omega \cdot cm^2$ with increased self-assembly time from 0 h to 12 h, and decreased to 259.7 $\Omega \cdot cm^2$ with assembly times longer than 12 h till 16 h. R_{ct} values decreased as a result of N-bda adsorption. This fact suggests that the inhibitor molecules may first be chemically adsorbed on the copper surface and cover some sites of the electrode surface. Then probably form molecular layers on the copper surface. These layers protect copper surface from attack by chloride ions. With the extension of self-assembly time, the self-assembled films released off, leaving the copper surface exposed to the solution. The corrosion rate increased, and the inhibition efficiency reduced. The results agree well with the date obtained by polarization and provide further confirmation of the ability of N-bda as a good inhibitor for copper corrosion in a 0.5 mol/L NaCl solution.

3.6 Research on the rule of the adsorption
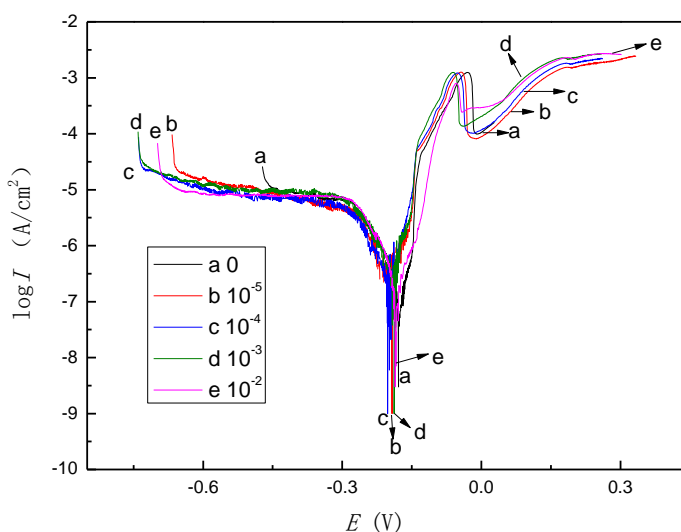
Figure 8. Polarization curves and the Langmiur adsorption plots for copper electrodes (self-assembly 12 h in different concentration of N-bda –ethanol solution) in a 0.5 mol/L NaCl solution at room temperature

The result of both EIS and polarization curve measurements indicated that the best self-assembly time was 12 h. The polarization curve measurements of copper electrodes self-assembled in different concentrations of N-bda-ethanol solution were carried out in a 0.5 mol/L NaCl solution at room temperature. The Tafel polarization curves exibites in Fig. 8a and the polarization measurement results are shown in Table 3. With the increase of the N-bda-ethanol concentration, the inhibition efficiency increased. When the self-assembled concentration was 1 mmol/L, j_{corr} was down to 0.0390 μA/cm^2, *IE* reached the highest value, was up to 98.2%. When the concentration was 0.01 mol/L, the inhibition efficiency was a litter lower than the *IE* value in the 1 mmol/L N-bda solution.

Table 3. Polarization measurement results for copper electrodes (self-assembly 12 h in different concentration of N-bda –ethanol solution) in a 0.5 mol/L NaCl solution

Concentration (mmol/L)	E_{corr} (mV)	j_{corr} (μA•cm^{-2})	θ	*IE*(%)
bare	-179.0	2.192		
0.01	-193.0	0.631	0.712	71.2
0.10	-202.0	0.376	0.829	82.9
1.00	-188.0	0.0390	0.982	98.2
10.00	-189.0	0.0476	0.978	97.8

The degree of surface coverage ($\theta = IE/100$) values were listed in Table 3. The values of θ were fitted into the Langmuir adsorption isotherm model [37], which has the form in Equation 3.

$$C_{(inh)}/\theta = 1/K_{ads} + C_{(inh)} \qquad (7)$$

where $C_{(inh)}$ is inhibitor concentration, θ is the degree of surface coverage, and K_{ads} is the equilibrium constant for the adsorption process. The plot of surface coverage (θ) as a function of N-bda concentrations at room temperature is shown in Fig. 7b. The straight line was obtained for N-bda suggested that its adsorption on the copper surface follows the Langmuir isotherm. The average value of K_{ads} calculated from equation 3 was 55.18 mol^{-1}. The high value of the adsorption equilibrium constant reflects the high value of adsorption ability of the inhibitor on the copper surface.

The value of Kads is used to calculate the standard free energy change (ΔG°_{ads}) accroding Equation 4.

$$\Delta G^{\circ}_{ads} = -RT\ln(55.5K_{ads}) \qquad (8)$$

where R is the universal gas constant and T is the absolute temperature. The value of ΔG°_{ads} was - 37 kJ/mol. The negative value of standard free energy of adsorption indicates spontaneous adsorption of the inhibitor on copper surface. The value of standard free energy was between - 40 and - 20 kJ/mol [38]. It can be concluded that the adsorption of N-bda molecules on the copper surface was in the form of physical and chemical adsorption.

4. CONCLUSIONS

Chemical and electrochemical measurements are used to study the capability of N-benzylidene-4-dodecylaniline to inhibit copper corrosion in a 0.5 mol/L NaCl solutions. The benzene ring and the

long chain in N-bda favour increase adsorption on the copper surface, which leads to increased inhibition efficiency value*s*. The highest inhibition efficiency of N-bda is achieved 98.2% within a self-assembly time of 12 h and in the concentration of 1 mmol/L N-bda, below or beyond which the inhibition efficiency decreased, as revealed by polarisation curve and impedance calculations. The results show clearly that N-bda is a new Schiff base that efficiently inhibits copper corrosion in a 0.5 mol/L NaCl solution. The adsorption form of N-bda molecules on the copper surface is physical and chemical adsorption.

References

1. K.F. Khaled, *Corros. Sci*. 52 (2010) 3225–3242.
2. M.M. Antonijevic, M.B. Petrovic, *Int. J Electrochem. Sci*. 1 (2008) 1–28.
3. Z. Li, L. Jin, W. Wang, S. Wang, *Int. J Electrochem. Sci*. 8 (2013) 6513–6523.
4. E.M. Sherif, A.A. Almajid, *J Appl. Electrochem*. 40 (2010) 1555–1562.
5. D.Q. Zhang, L.X. Gao, G.D. Zhou, K.Y. Lee, *J Appl. Electrochem*. 38 (2008) 71–76.
6. S.R. Gupta, P. Mourya, M.M. Singh, V.P.Singh, *J. Organomet. Chem*. 767(2014) 136–143.
7. R. Solmaz, G. Kardas, B. Yazıcı, M. Erbil, *Colloids Surf. A: Physicochem. Eng. Aspects* 312 (2008) 7–17.
8. T.J. Mullen, A.A. Dameron, A.M. Andrews, P.S. Weiss, *Aldrichim. Acta* 40 (2007) 21–31.
9. E.M. Sherif, R.M. Erasmus, J.D. Comins, *J Colloid Interface Sci*. 306 (2007) 96–104.
10. R. Solmaz, *Corros. Sci*. 52 (2010) 3321–3330.
11. O.K. Abiola, N.C. Oforka, S.S. Angaye, *Mater. Lett*. 58 (2004) 3461–3466.
12. D.Q. Zhang, L.X. Gao, G.D. Zhou, H.G. Joo, K.Y. Lee, *J Appl. Electrochem*. 2011, 41, 491–498.
13. D.Q. Zhang, L.X. Gao, G.D. Zhou, *J Appl. Electrochem*. 35 (2005) 1081–1085.
14. Y.Y. Feng, S.H. Chen, W.J. Guo, Y.X. Zhang, G.Z. Liu, *J Electroanal* Chem. 602 (2007) 115–122.
15. P. Zhao, Q. Liang, Y. Li, *Electrochemical, Appl. Surf. Sci*. 252 (2005) 1596– 1607.
16. A.A. Gürten, M. Erbil, K. Kayakirilmaz, *Cem. Concr. Compos*. 27 (2005) 802–808.
17. C.A. Gonzalez-Rodriguez, F.J. Rodriguez-Gomez, J. Genesca-Llongueras, *Electrochim. Acta* 54 (2008) 86–90.
18. A. Mezzi, E. Angelini, T. De Caro, S. Grassini, F. Faraldi, C. Riccuccia, G. M. Ingoa, *Surf. Interface Anal*. 44 (2012) 968–971.
19. X.Y. Liu, S.H. Chen, H.Y. Ma, G.Z. Liu, L.X. Shen, *Appl. Surf. Sci*. 253 (2006) 814–820.
20. K.R. Ansari, M.A. Quraishi, *Journal of Industrial and Engineering Chemistry*, 20(2014)2819–2829.
21. N S. Thirugnaselvi, S. Kuttirani, A.R.Emelda, *Trans. Nonferrous Met. Soc. China* 24(2014) 1969−1977..
22. M. Behpour, S.M. Ghoreishi, N. Soltani, M. Salavati-Niasari, *Corros. Sci*. 51 (2009) 1073–1082.
23. K.C. Emregul, E. Duzgun, O. Atakol, *Corros. Sci*. 48 (2006) 3243–3260.
24. Q. Qua, Z.Z. Hao, L. Li, Wei Bai, Y.J. Liu, Z.T. Ding, *Corros. Sci*. 51 (2009) 569–574.
25. K.C. Emregul, M. Hayvali, *Corros. Sci*. 48 (2006) 797–812.

26. I. Ahamad, C. Gupta, R. Prasad, M.A. Quraishi, *J Appl. Electrochem.* 40 (2010) 2171–2183.
27. J. Zhang, W.Z. Yu, Y.G. Yu, L.J. Yu, Z.J. Ren, *Acta Phys. Chim. Sin*. 26 (2010) 1385–1390.
28. A. Yildirim, M. Cetin, *Corros. Sci*. 50 (2008) 155–165.
29. A. Frignani, F. Zucchi, G. Trabanelli, V. Grassi, *Corros. Sci.* 48 (2006) 2258–2273.
30. J. Zhang, S.Q. Hu, Y. Wang, W.Y. Guo, J.X. Liu, L. You, *Acta Chim. Sin*. 66 (2008) 2469–2475.
31. D.G. Li, S.H. Chen, S.Y. Zhao, H.Y. Ma, *Colloids Surf*. 273 (2006) 16–23.
32. N.A. Negm, Y.M. Elkholy, M.K. Zahran, S.M. Tawfik, *Corros. Sci*. 52 (2010) 3523–3536.
33. M.G. Hosseini, M.R. Arshadi, *Int J Electrochem. Sci*. 4 (2009) 1339–1350.
34. Z. Zhang, S.H. Chen, Y.H. Li, S.H. Li, L. Wang, *Corros. Sci.* 51 (2009) 291–300.
35. H.Y. Ma, C. Yang, S.H. Chen, Y.L. Jiao, S.X. Huang, D.G. Li, J.L. Luo, *Electrochim. Acta* 48 (2003) 4277–4289.
36. K.F. Khaled, M.A. Amin, N.A. Al-Mobarak, *J Appl. Electrochem*. 40 (2010) 601–613.
37. M. Sahin, S. Bilgic, H. Yilmaz, *Appl. Surf. Sci*. 195 (2002) 1–7.
38. A. Doner, R. Solmaz, M. Ozcan, G. Kardas, *Corros. Sci*. 53 (2011) 2902–2913.